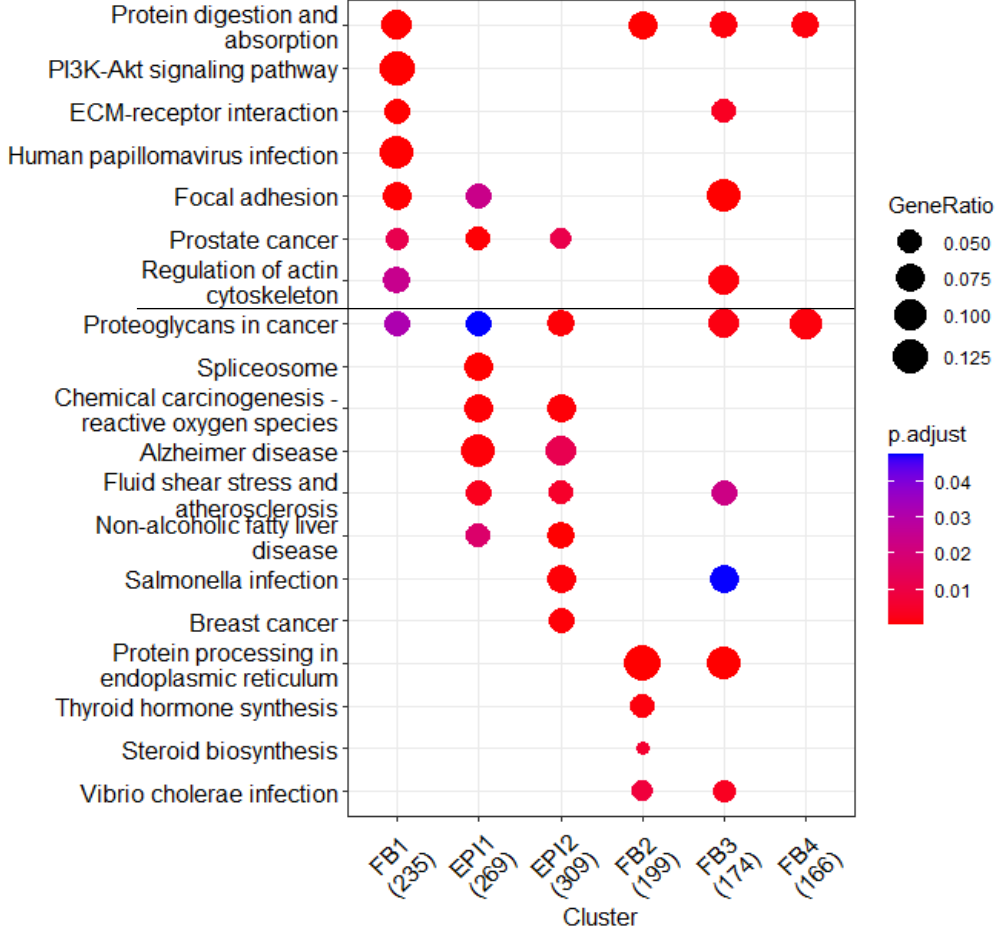


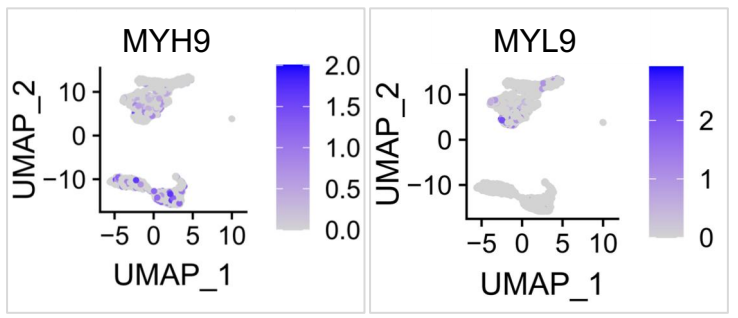
Figure S1. Skin cyst structure.

- A. H&E staining and Vimentin immunostaining show that epithelial cysts in mouse skin are surrounded by layers of dermal cells.
- B. H&E staining shows that the layers of dermal cells surrounding the epidermal aggregate are significantly increased from D1 to D3.
- C. K14 immunostaining shows that the layers of dermal cells surrounding the epidermal aggregate are significantly increased from D1 to D3.
- D. Laminin and Col IV immunostaining shows the dermal cells are attached to the basement membrane.
- E. P-cadherin and Col VII immunostaining shows the epidermal aggregate polarizes from D1 to D3.
- F. Schematic of dermal cell stretching epidermal cell by observing live-imaging of FVB-GFP mouse cells. The analysis was based on the movies published in our previous study (1).
- G. Vimentin and K14 immunostaining shows that dermal cells attach to the epidermal cyst in newborn and adult mouse skin organoids, and hair regeneration from the newborn and adult organoid cultures. N = 3, **p < 0.01.
- H. Wholemout immunostaining and transplantation assay show recombination of newborn and adult cells in organoid cultures results in differential hair regeneration. N, newborn cells. A, adult cells. Epi, E, epidermal cells. D, dermal cells.

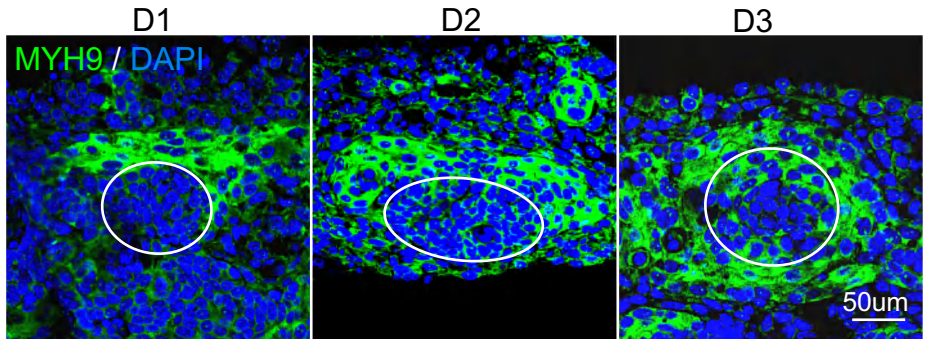
A Mechanical signaling pathway in dermal cells by scRNA-seq



B scRNA-seq of MYH9 and MYL9 expression in D48 human skin organoid



C MYH9 expression during skin organoid culture



D MYL9 expression during skin organoid culture

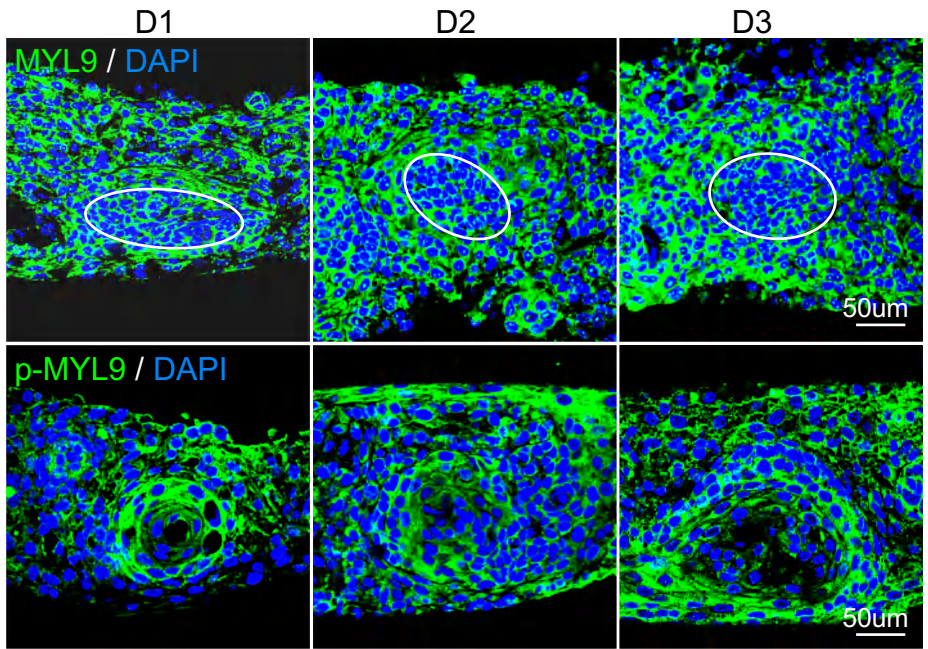


Figure S2. scRNA-seq shows mechanical signaling pathway in dermal cells in human skin organoid culture.

- A. KEGG analysis shows Regulation of the actin cytoskeleton in dermal cells (FB1 and FB3).
- B. UMAP plots of MYH9 and MYL9 expression in epidermal and dermal clusters by unbiased clustering.
- C. Immunostaining shows MYH9 expression during skin organoid culture.
- D. Immunostaining shows MYL9 and p-MYL9 expression during skin organoid culture.

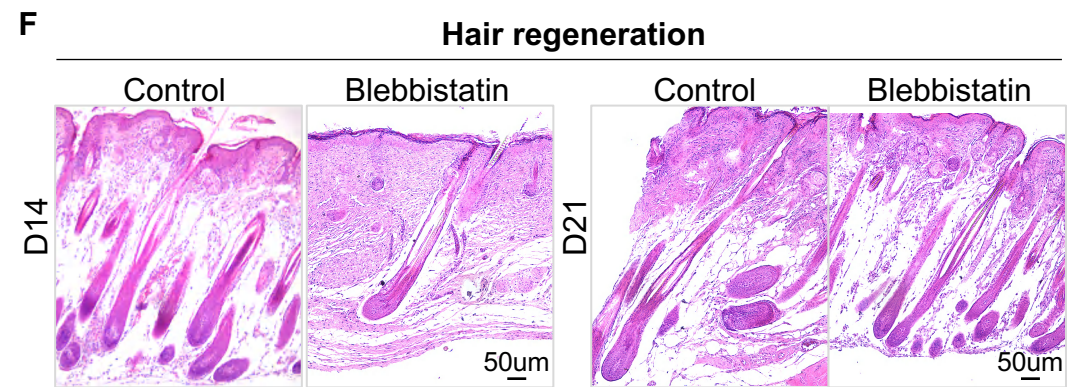
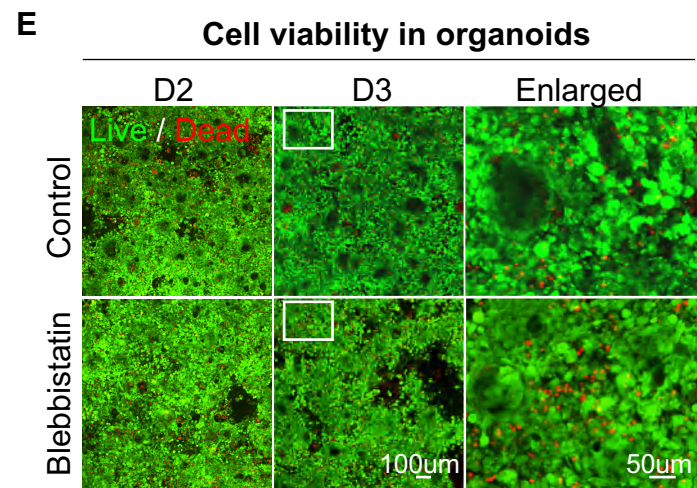
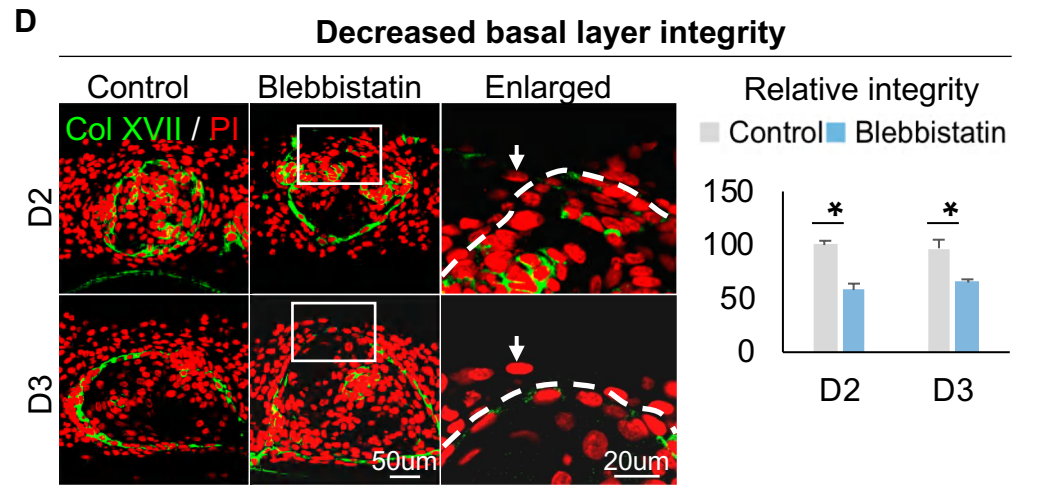
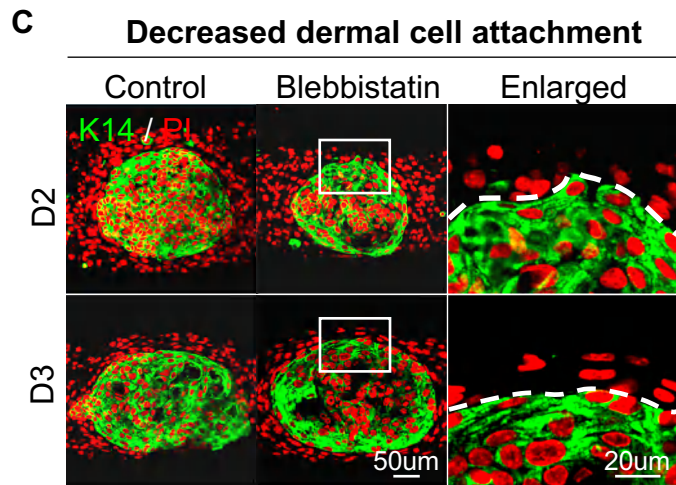
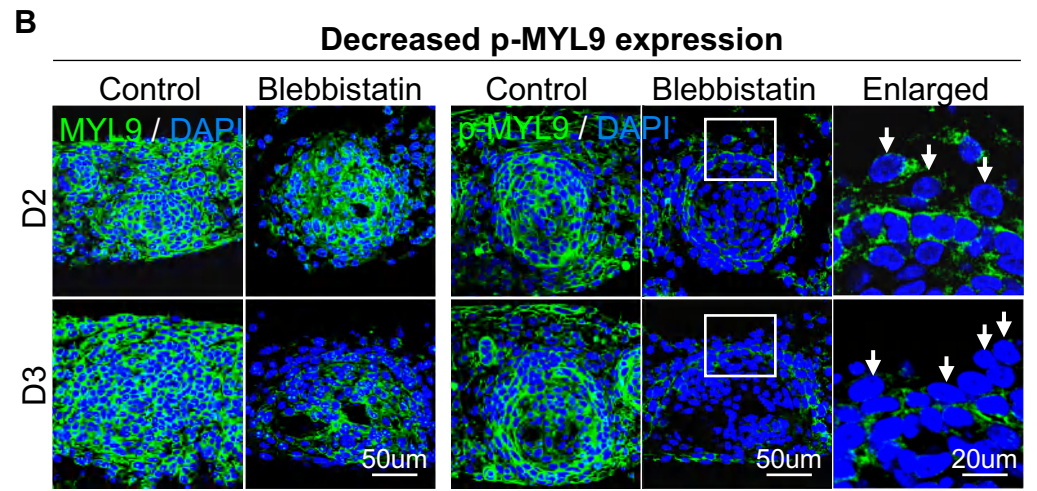
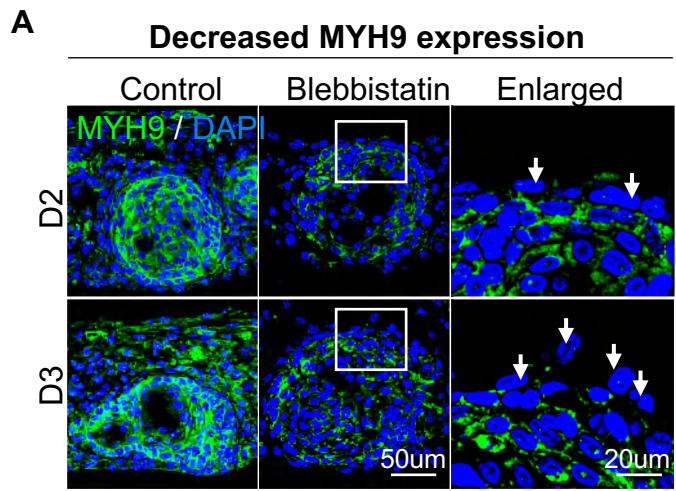
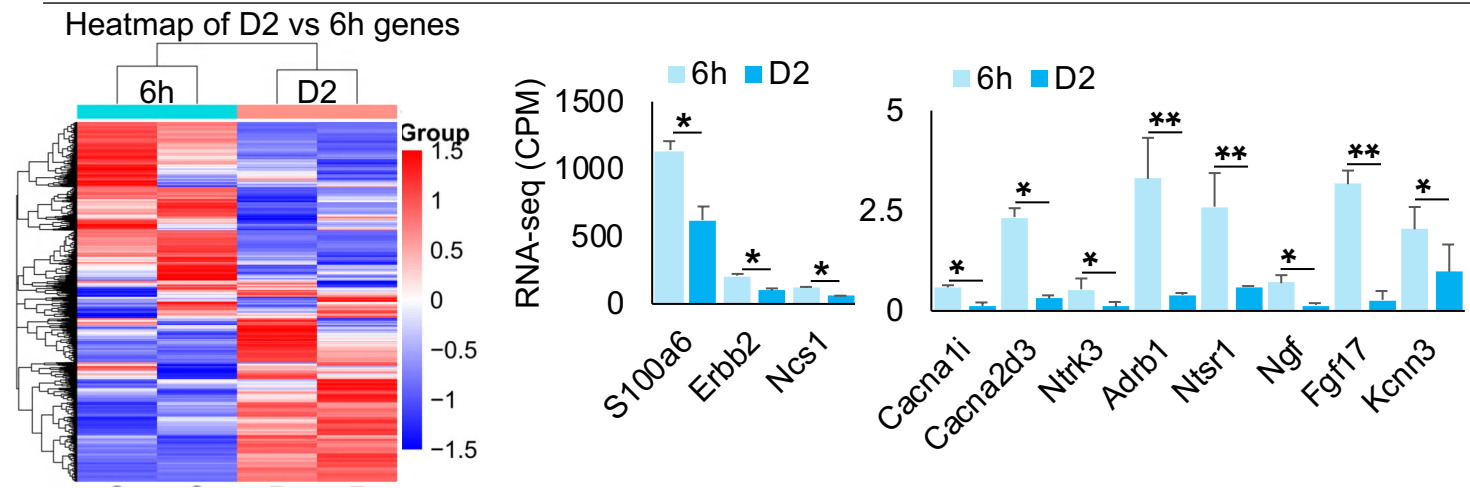


Figure S3. The decreased dermal cell attachment in skin organoid culture after treatment of Blebbistatin.

- A. Immunostaining show MYH9 expression in Blebbistatin-treated cultures.
- B. Immunostaining show MYL9 and p-MYL9 expression in Blebbistatin-treated cultures.
- C. K14 immunostaining shows dermal cell attachment after treatment of Blebbistatin.
- D. Collagen XVII immunostaining shows basal layer integrity after treatment of Blebbistatin (left). Statistics of the basal layer integrity (right). $N \geq 3$, $*p < 0.05$, and # no significant change.
- E. Live-Dead staining shows cell survival after treatment of Blebbistatin.
- F. H&E staining shows the hair cycle in the skin regenerated by the transplantation of Blebbistatin-treated cultures.

A RNA-seq analysis of Ca²⁺ pathway gene expression in D2 vs 6h cultures



B Blebbistatin treatment did not affect Ca²⁺ concentration

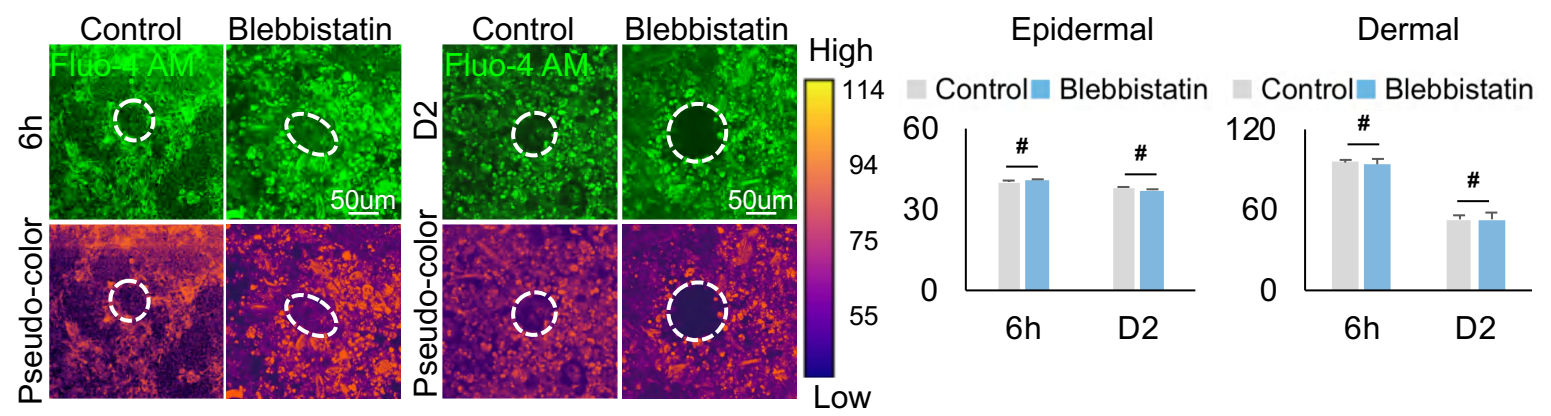
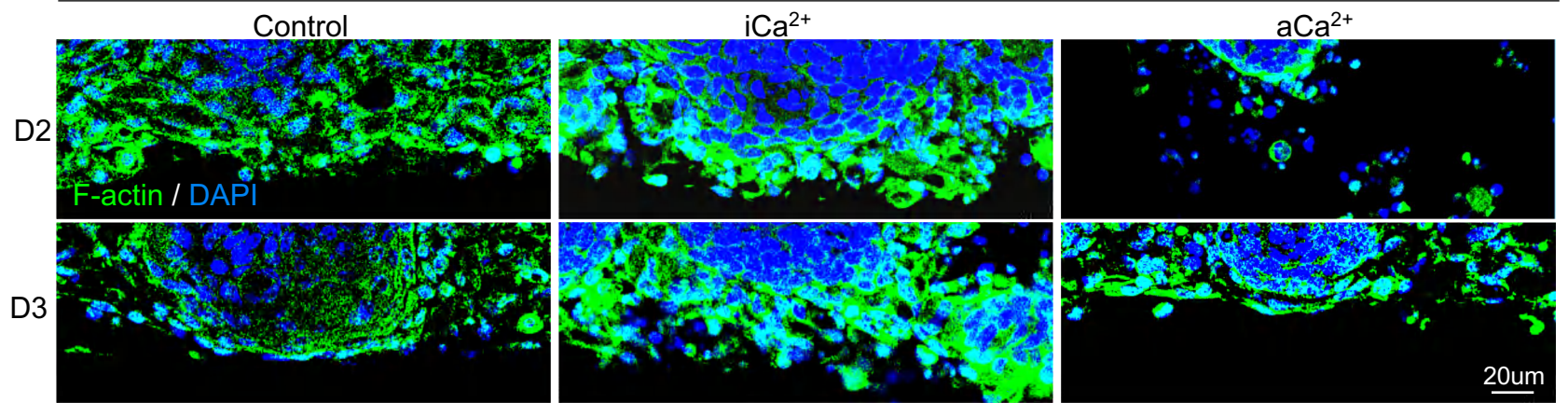


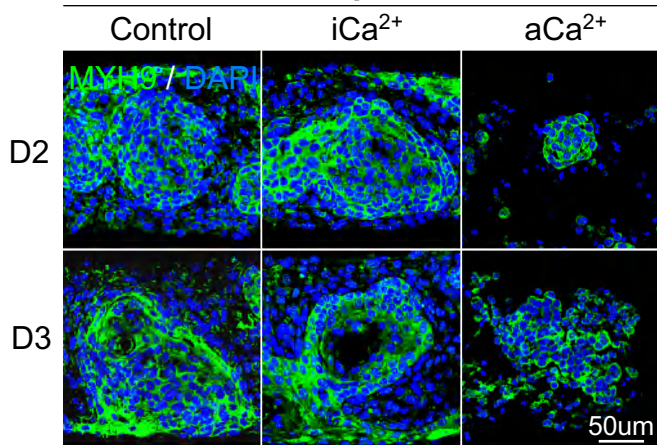
Figure S4. Bulk RNA-seq analysis shows Calcium pathway gene expression in 6h and D2 skin organoid culture.

- A. Hierarchical clustering shows differential gene expression at D2 vs 6h (left). RNA-seq analysis of calcium pathway genes that are differentially expressed at D2 vs 6h (right).
- B. Fluo-4 AM fluorescent probe detection assay and statistics show Ca²⁺ concentration within Blebbistatin cultures at 6h and D2. N ≥ 3, # no significant change.

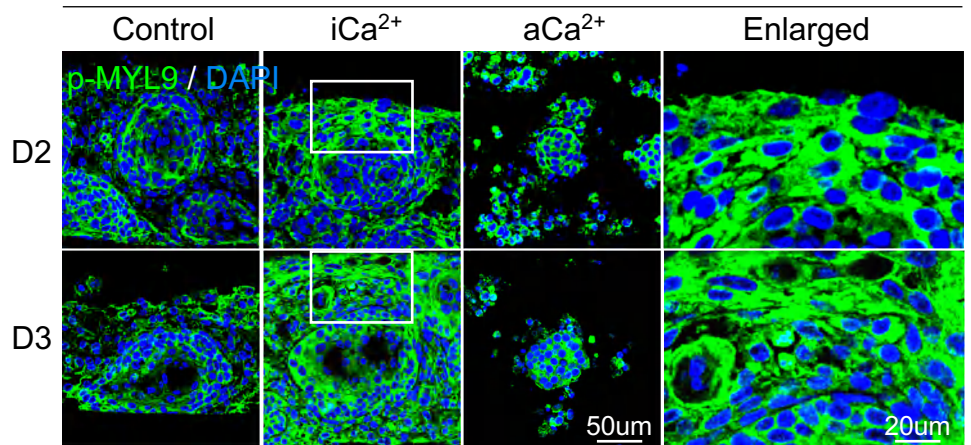
A Ca²⁺ disturbed F-actin arrangement in dermal cells



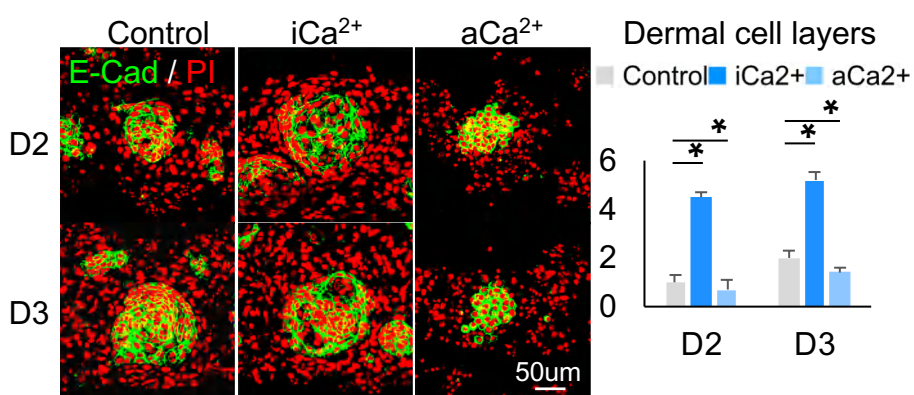
B Blocking Ca²⁺ did not affect MYH9 expression



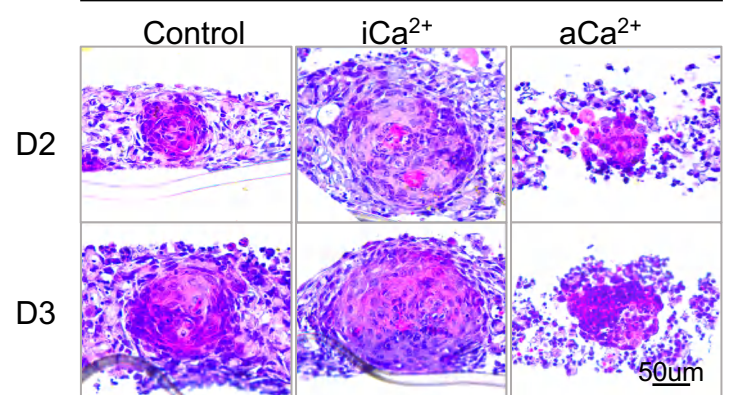
C Blocking Ca²⁺ induced p-MYL9 expression in dermal cells



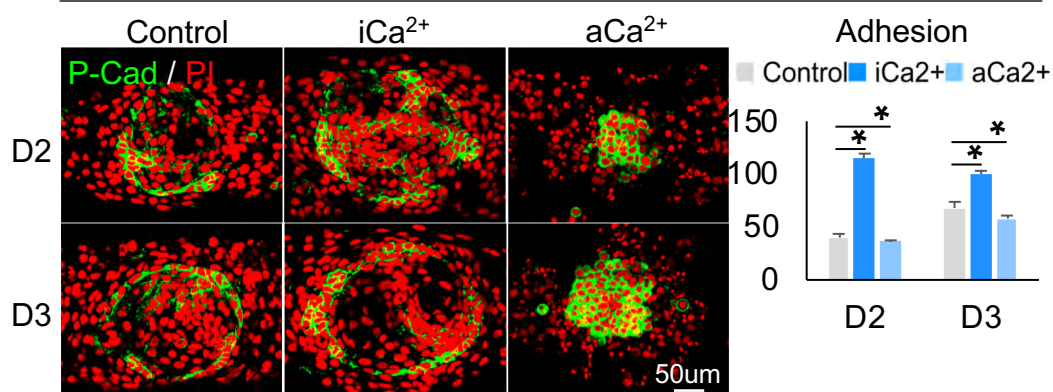
D Blocking Ca²⁺ induced dermal cell attachment



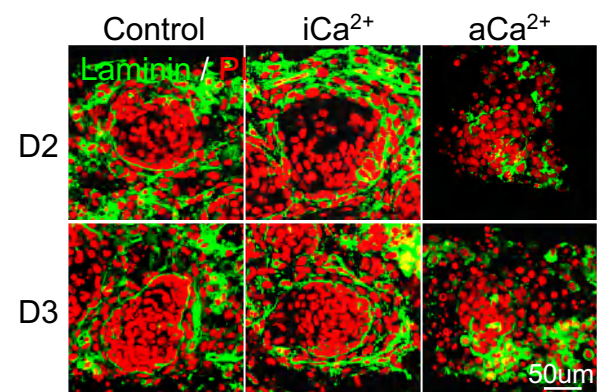
E Activating Ca²⁺ resulted in smaller epidermal cyst size



F Blocking Ca²⁺ induced more epidermal adhesion



G Blocking Ca²⁺ induced basement membrane formation



H Hair regeneration

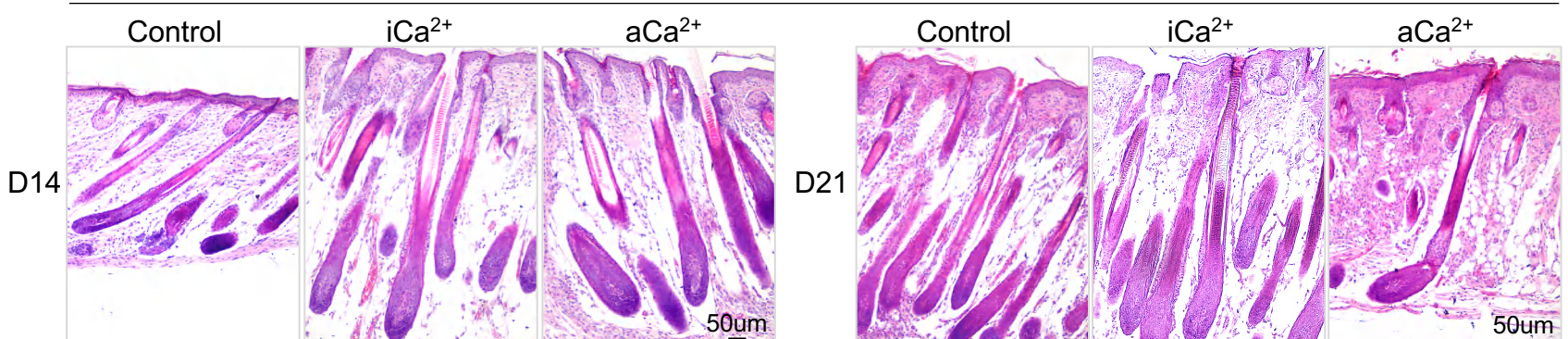


Figure S5. Calcium influences dermal cell attachment.

- A. Enlarged views of immunostaining show F-actin arrangement after treatment with thapsigargin or ruthenium red.
- B. Immunostaining shows MYH9 expression in thapsigargin- or ruthenium red-treated cultures.
- C. Immunostaining shows MYL9 and p-MYL9 expression in thapsigargin- or ruthenium red-treated cultures.
- D. E-Cadherin immunostaining shows more dermal cell attachment after blocking or activating the calcium signaling.
Statistics of the dermal layers surrounding the epidermal cyst after treatment.
- E. H&E staining shows a larger epidermal cyst in size after blocking calcium signaling.
- F. P-Cadherin immunostaining shows higher multipotency after blocking or activating the calcium signaling. $N \geq 3$, $*p < 0.05$, and # no significant change.
- G. Laminin immunostaining shows that blocking the calcium signaling promotes basement membrane formation.
- H. H&E staining shows the hair cycle in the skin regenerated by the transplantation of the calcium signaling-blocked or activated cultures.

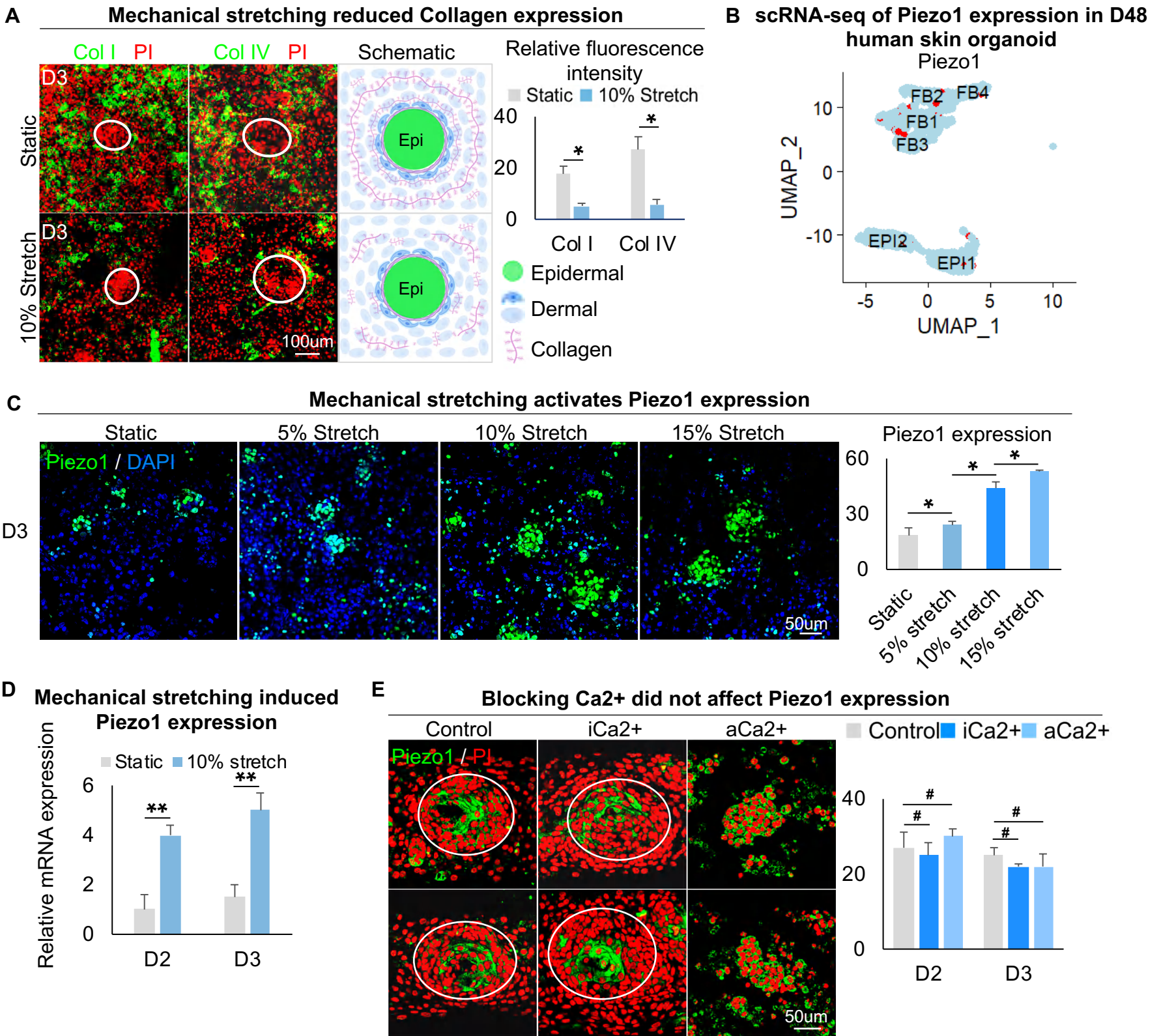


Figure S6. Mechanical stretching inhibits Collagen expression but induces Piezo1 expression.

- A. Collagen I and Collagen IV immunofluorescence staining shows 10% mechanical stretching reduced Collagen expression. Schematic of Collagen expression after flexcell mechanical stretching.
- B. UMAP plots of Piezo1 expression in epidermal and dermal clusters by unbiased clustering.
- C. Immunostaining and statistics show that mechanical stretching induced Piezo1 expression under Static, 5%, 10%, or 15% Stretch.
- D. Quantitative RT-PCR shows that the application of 10% mechanical stretching enhanced the expression of Piezo1 in skin organoid culture.
- E. Immunostaining and statistical analysis show Piezo1 expression after blocking or activating the calcium signaling. $N \geq 3$, ** $p < 0.01$, * $p < 0.05$, and # no significant change.

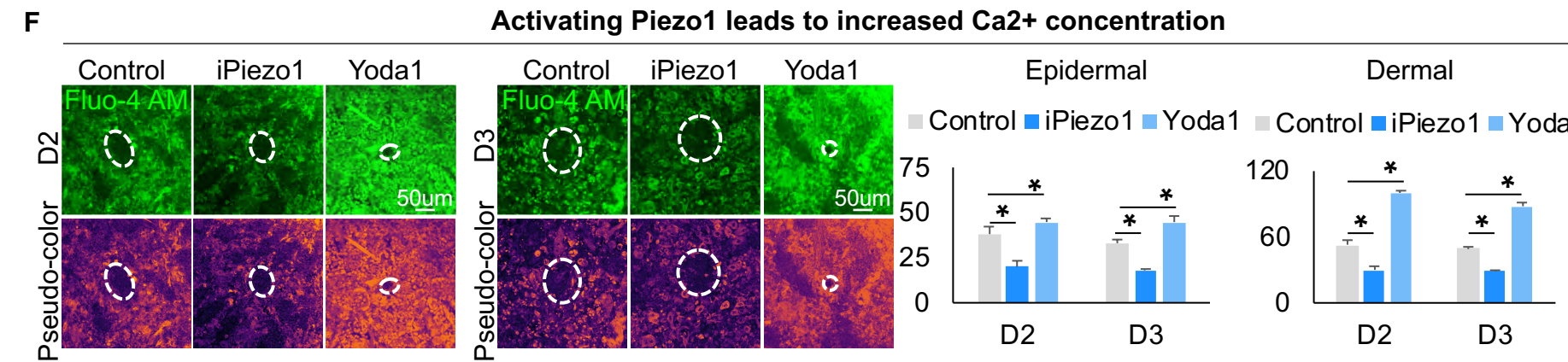
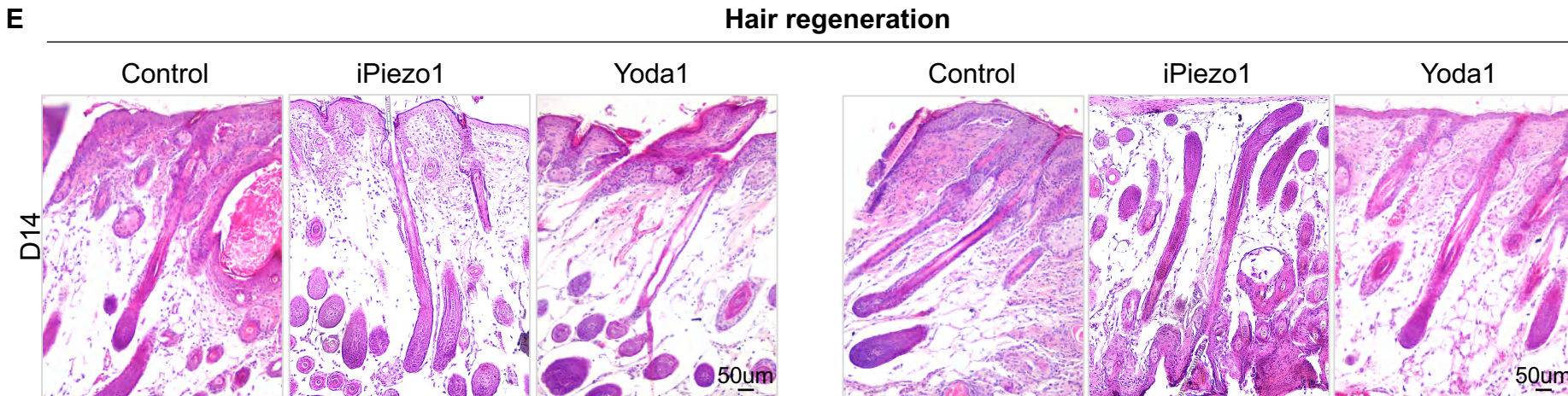
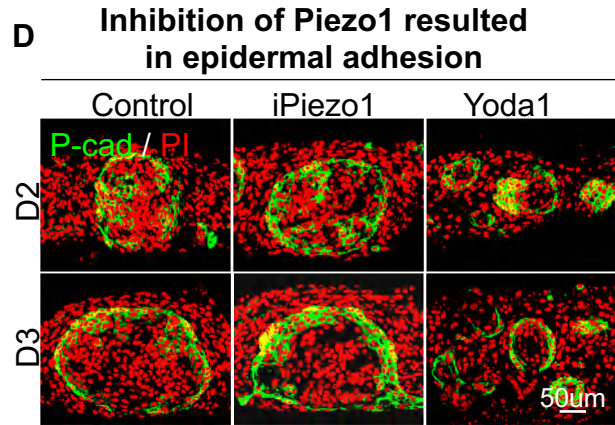
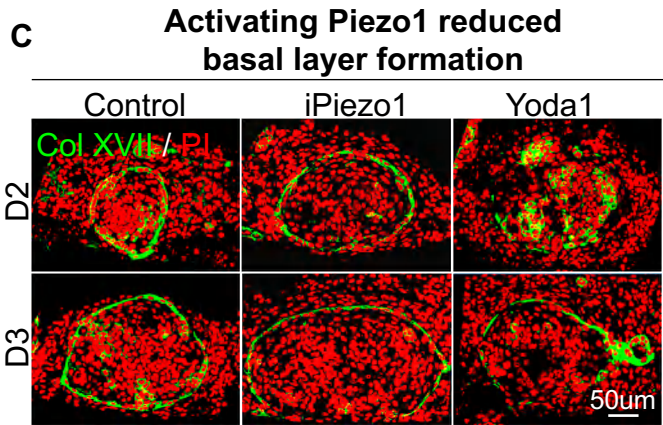
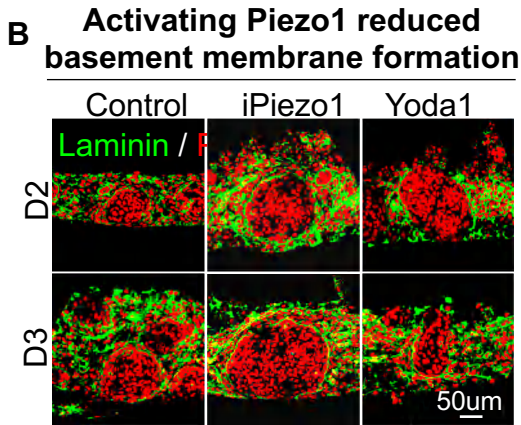
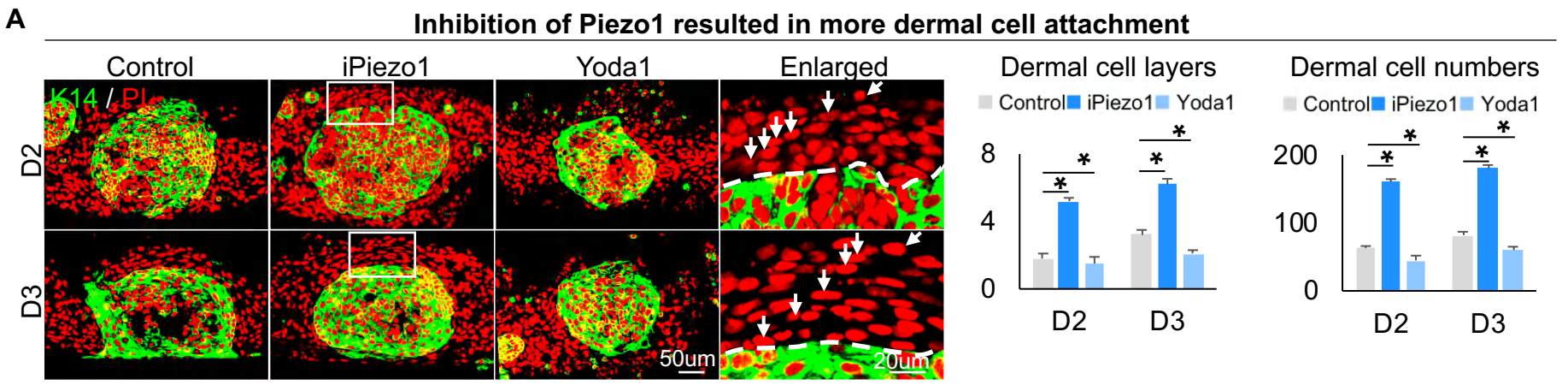


Figure S7. Piezo1 inhibits dermal cell attachment to the epidermal cysts.

- A. K14 immunostaining shows more dermal cell attachment after blocking Piezo1. Statistics of the dermal layers and dermal cells surrounding the epidermal cyst after treatment.
- B. Laminin immunostaining shows that blocking the Piezo1 promotes basement membrane formation.
- C. Collagen XVII immunostaining shows that blocking the Piezo1 promotes basal layer formation.
- D. P-Cadherin immunostaining shows higher multipotency after blocking Piezo1.
- E. H&E staining shows the hair cycle in the skin regenerated by the transplantation of the Piezo1-blocked or activated cultures.
- F. Ca²⁺ concentration was detected by the Fluo-4 AM fluorescent probe within Piezo1 inhibitor (GsMTx4 TFA) or Piezo1 activator (Yoda1) cultures at D2 and D3. N ≥ 3, *p < 0.05, and # no significant change.

Table S1. Sequences of the Real-time qPCR.

RT-qPCR Primers		
Gene Name	Forward	Reverse
Piezo1	ACCAGTTTCTGGGACAAAACG	CCAGCCTGGTGGTGTAAAGA
GAPDG	AGGTCGGTGTGAACGGATTG	TGTAGACCATGTAGTTGAGGTCA

Table S2. Antibodies used in this study.

Antibody	Isotype	Company	Cat #
KRT14	Rabbit	Boster	A01432
Collagen I	Goat	Arigobio	ARG21965
Collagen IV	Rabbit	Abcam	ab19808
Collagen VII	Rabbit	Abcam	ab93350
Collagen XVII	Rabbit	Beyotime	AF1078
P-Cadherin	Goat	R&D	AF761
E-Cadherin	Mouse	Beyotime	AF0138
Laminin	Rabbit	Abcam	ab11575
Piezo1	Rabbit	Affinity	DF12083
MYL9	Rabbit	Proteintech	15354-1-AP
p-MYL9	Rabbit	Bioss	bs-4060R
MYH9	Rabbit	Beyotime	AF7536
F-actin	N/A	Invitrogen	A12379

Table S3. Small molecule inhibitors and activators used in this study.

Cat #	Product Description	IC ₅₀
SF9087	Blebbistatin (myosin II inhibitor)	IC ₅₀ = 0.5 μM-5 μM for inhibiting several striated muscle myosins as well as vertebrate nonmuscle myosin IIA and IIB.
HY-103311	Ruthenium Red (Calcium inhibitor)	IC ₅₀ = 7 μM for attenuating capsaicin-induced cation channel opening.
SC0389	Thapsigargin (Calcium activator)	IC ₅₀ =30 nM for increasing in cytosolic calcium results from the specific inhibition of endoplasmic reticulum Ca ²⁺ -ATPases.
S7399	GsMTx4 TFA (Piezo1 inhibitor)	GsMTx4 TFA (5 μM) reduces Piezo1-mediated charge transfer to 38% of its initial levels in HEK293 cells transfected with Piezo1 cDNA.
GC18233	Yoda1 (Piezo1 activator)	EC ₅₀ =17.1 μM, it is a potent and selective Piezo1 agonist.